An Excited-State-Specific Pseudoprojected Coupled-Cluster Theory

Harrison Tuckman[1] and Eric Neuscamman[1,2,a)]
[1)] *Department of Chemistry, University of California, Berkeley, California 94720, USA*
[2)] *Chemical Sciences Division, Lawrence Berkeley National Laboratory, Berkeley, CA, 94720, USA*

(Dated: 6 September 2023)

We present an excited-state-specific coupled-cluster approach in which both the molecular orbitals and cluster amplitudes are optimized for an individual excited state. The theory is formulated via a pseudoprojection of the traditional coupled-cluster wavefunction that allows correlation effects to be introduced atop an excited state mean field starting point. The approach shares much in common with ground state CCSD, including size extensivity and an N^6 cost scaling. Preliminary numerical tests show that, when augmented with N^5-cost perturbative corrections for key terms, the method can improve over excited-state-specific second order perturbation theory in valence, charge transfer, and Rydberg states.

I. INTRODUCTION

Mean field methods such as Hartree-Fock (HF) theory[1] are useful for creating qualitatively correct depictions of a molecules' electronic structure, but the finer details of electron correlation must also be addressed in order to achieve quantitative energy predictions. When working with ground state molecules near their equilibrium geometries, wavefunction methods traditionally capture this correlation by hierarchically applying perturbation based and/or coupled-cluster (CC) based corrections to the HF wavefunction.[2–5] An especially noteworthy part of this hierarchy is coupled-cluster with singles, doubles, and perturbative triples (CCSD(T)),[6,7] which is often referred to as the "gold standard" thanks to its ability to deliver sub-k_BT accuracy at polynomial cost in a variety of chemically important settings.[8–10] In practice, of course, wavefunction methods are often eschewed in favor of the more computationally efficient density functional theory (DFT),[11–14] but, one way or another, accurate chemical predictions rely on correctly accounting for the effects of electron correlation.

Achieving quantitative predictions in electronically excited states becomes more complicated, as methods must now contend with open-shell spin-recombination, post-excitation orbital relaxations, and the effects of these on the details of electron correlation. In practice, many of the most widely used excited state methods such as time-dependent DFT (TD-DFT)[15–17], and linear response CC (LR-CC)[18,19] approach excited states by way of linear response theory. Equation-of-motion CC (EOM-CC),[20–22] which is often motivated from a lens not rooted explicitly in linear response theory, ends up bearing many similarities to LR-CC, including matching excitation energies.[19,23] Though LR-CC and EOM-CC differ for some other properties such as transition moments, the primary focus of this paper is excitation energies, and so we will simply refer to both these theories as linear response approaches. While all of these linear response CC approaches capture open-shell singlet character and have a long record of success, they are not without their difficulties. Typically, the linear response approximation requires the assumption that key aspects of the electronic structure are shared between ground and excited states. For example, much of the correlation treatment in EOM-CC and LR-CC comes from the shared exponential operator. Likewise, the widely used adiabatic approach to TD-DFT retains the same orbital shapes for all spectator electrons, regardless of how substantially an excitation has changed the electrostatic environment that these electrons sit in. These assumptions can be problematic in situations involving large and thus nonlinear post-excitation relaxations, such as many charge transfer, Rydberg, core, and double excitations.[24–38] Linear response methods can also struggle in situations where the ground state is not well described by mean field theory, as they can inherit the ground state difficulties even if the structure of the excited state is simple. While there are many different corrections and augmentations that can be added to these methods in order to address specific shortcomings – e.g. long range corrections in TD-DFT[39,40] or charge transfer separability corrections in EOM-CCx[41] – the various challenges facing linear response methods have prevented the community from coalescing around a unifying "gold standard" and have left excited state modeling at a distinct disadvantage relative to ground states.

Motivated in part by the limitations of linear response, there has been much recent work on excited-state-specific methods. Whether studying single determinant wavefunctions,[42–46] configuration interaction (CI) wavefunctions,[47] CC wavefunctions,[48–54] or DFT functionals,[55–57] the theme of locating higher energy, state-specific excited state and open-shell roots is becoming increasingly prevalent across the field. Recognizing that, in the ground state, CCSD is a crucial stepping stone towards CCSD(T) as well as a useful method in its own right, our focus here is to construct a CCSD-like excited-state-specific CC theory atop an excited state mean field (ESMF) starting point[58–60] that, like HF in

[a)] Electronic mail: eneuscamman@berkeley.edu

the ground state, has already taken care of state-specific orbital relaxations. Besides, with an N^5 cost ESMF-based second order perturbation theory (ESMP2) already established,[61] the longstanding pattern in ground state correlation methods makes it seem natural to expect an N^6 cost CC method to provide the next step in a hierarchy of excited-state-specific correlation methods.

Creating this CC method poses immediate challenges, however, due to the inherently multireference nature of excited states, and so it is prudent to consider the pros and cons of existing approaches to multireference CC theory. Such methods typically fall into one of three categories: the Jeziorski-Monkhort (JM) based methods, the internal contraction (ic) based methods, and the single-reference based methods.[62–64] While research continues into notable multi-reference coupled-cluster methods which make use of the Jeziorski-Monkhorst ansatz such as State-Universal (SU)-MRCC,[65–67] Brilluoin-Wigner (BW)-MRCC,[68,69] single root (sr)-MRCC,[70,71] Mukherjee (Mk)-MRCC,[72,73] MRexpT,[74] and two-determinant (TD)-CC,[75–77] as well as methods which make use of internally contracted schemes such as multiple flavors of ic-MRCC,[78–80] partially internally contracted (pIC)-MRCC,[81] and block correlated CC,[82] these methods are not without their difficulties. In general, the state-universal JM methods can face numerical instabilities due to the intruder state problem,[64] while the state-specific approaches have an inherent mismatch between the number of cluster amplitudes and residual equations.[62,63] Furthermore, both of these methods lack an invariance to orbital rotations within the active space,[83,84] making the final energy dependent on the choice of orbitals. Meanwhile, the internally contracted methods must contend with both overlap matrices that can introduce their own numerical instabilities and, in some cases, approximate truncations of nonterminating BCH expansions.[62–64,85,86]

To avoid these challenges and maintain as much of the convenience of single-reference CC as possible, we will therefore attempt to tackle multi-reference character via an approach similar to the "little t" and "little tq" methods,[87–93] which rely on a selective inclusion of only a subset of triples and/or quadruples. The subset in question has often been identified by defining an active space, but more recent work has also explored more general approaches.[94,95] In a manner similar to the N^5 variant of ESMP2,[61] we propose to use the ESMF starting point to automatically identify a subset of triples to include, thus limiting the number of triples in a way that makes an N^6 scaling possible and avoids user-defined active spaces. With the introduction of a projection-like operator that suppresses the Aufbau configuration while maintaining size extensivity and intensivity, and with the help of a substantial dose of automated algebra, we find that this approach leads to a fully excited-state-specific, CCSD-like theory for adding CC-style correlation to an ESMF starting point.

II. THEORY

A. Conventional Ground State Coupled-Cluster

While there exist a plethora of resources illustrating ground state coupled-cluster theory in extensive detail,[5,96,97] we wish to provide a quick summary here so that we may draw parallels between our excited state method and the ground state theory. Although CC theory is at its heart an approximation to the many-body energy, it can be motivated by a wavefunction that is defined by operating the exponential of a cluster operator, $\hat{T}$, on a reference, $|\phi_0\rangle$, which is most often the Hartree-Fock determinant,

$$|\psi\rangle = e^{\hat{T}}\,|\phi_0\rangle = \left(1 + \hat{T} + \frac{1}{2}\hat{T}^2 + \dots\right)|\phi_0\rangle\,. \tag{1}$$

One of the challenges in applying this exponential operator is that obtaining a variational solution for the energy necessitates either exponentially scaling computational cost or an approximate truncation of the exponential expansion. Therefore, what is often done in practice is to utilize a projective approach where cluster amplitudes are determined by satisfying the eigenvector condition for the similarity transformed Hamiltonian in a chemically relevant subspace. For example, in CC with single and double excitations (CCSD), $\hat{T}$ is truncated to include only $\hat{T}_1$ and $\hat{T}_2$ while projections are taken against the reference determinant, $|\phi_0\rangle$, and all singly and doubly excited determinants, $|\phi_i^a\rangle$ and $|\phi_{ij}^{ab}\rangle$, in order to define an approximate (and non-variational) energy equation and a set of amplitude equations that can be solved to determine $\hat{T}_1$ and $\hat{T}_2$.[5,96,97]

$$E_{CCSD} = \langle\phi_0|\, e^{-(\hat{T}_1+\hat{T}_2)}\hat{H}e^{\hat{T}_1+\hat{T}_2}\,|\phi_0\rangle\,, \tag{2}$$

$$0 = \langle\phi_i^a|\, e^{-(\hat{T}_1+\hat{T}_2)}\hat{H}e^{\hat{T}_1+\hat{T}_2}\,|\phi_0\rangle\,, \tag{3}$$

$$0 = \langle\phi_{ij}^{ab}|\, e^{-(\hat{T}_1+\hat{T}_2)}\hat{H}e^{\hat{T}_1+\hat{T}_2}\,|\phi_0\rangle\,. \tag{4}$$

Here and in the rest of this paper, $i, j, k, \dots$ represent occupied spin orbitals while $a, b, c, \dots$ represent virtual spin orbitals relative to the reference. Solving the above equations produces the energy and cluster amplitudes, which can in turn be used to evaluate other properties.[5]

B. A Suitable Reference and the Usefulness of a Pseudoprojector

As is the case for the ground state, choice of a reference is the first step in our CC method. For studying electronically excited states, we elect to use the Excited State Mean Field (ESMF) method,[58–60] which is an excited state analog to the mean field HF reference, as a starting point. In a spin orbital basis, the ESMF wavefunction

Wavefunction	Description	Equation	MO Basis
$\|\phi_0\rangle$	RHF	—	RHF
$\|\phi_0^*\rangle$	ESMF Aufbau Formal Reference	5	ESMF TOP
$\|\psi_{ESMF}\rangle$	ESMF	5	ESMF TOP
$\|\psi_0\rangle$	Truncated ESMF Reference	6	ESMF TOP
$\|\Psi\rangle$	ESPCC	7	ESMF TOP

Table 1. A brief summary of the wavefunctions discussed in this paper, a short description of what they represent, the relevant equation where they are defined, and the MO basis they are constructed in.

can, if we neglect the possibility of the Aufbau determinant participating in the excited state, be expressed as

$$|\psi_{ESMF}\rangle = e^{\hat{X}} \left(\sum_{ia} c_{ia} \hat{a}_a^\dagger \hat{a}_i \, |\phi_0\rangle \right) = \sum_{ia} c_{ia} \hat{a}_a^\dagger \hat{a}_i \, |\phi_0^*\rangle \, . \tag{5}$$

Here $e^{\hat{X}}$ is an orbital rotation operator and $\hat{a}_a^\dagger$ and $\hat{a}_i$ are second quantization creation and destruction operators respectively. To arrive at the expression on the right of equation 5, the orbital rotation operator is acted on the original canonical orbital basis in order to result in a new basis whose orbitals are optimized for the specific excited state of interest. We denote this new basis with an asterisk, such that the Aufbau determinant in this ESMF orbital basis is denoted as $|\phi_0^*\rangle$. Immediately it is evident that our reference is a multi-determinant wavefunction, which can complicate CC methods.[62,64] We can mitigate the extent of the multireference nature of our wavefunction by performing a singular value decomposition (SVD) on the CI coefficients of the ESMF wavefunction and transforming our basis to a transition orbital pair (TOP) basis.[61] In the TOP basis — which shares many similarities with the natural transition orbital basis[98] and has been employed by methods such as EOM CC to reduce computational scaling[99] — each occupied index becomes paired with a virtual index, thereby reducing the number of determinants in our ESMF wavefunction. We can further reduce the number of determinants by truncating the ESMF wavefunction after a specified threshold. Although we will discuss generalizations below, in this initial investigation we choose to employ the most aggressive truncation scheme possible by truncating after the first singular value. For now, this results in our (renormalized) truncated ESMF reference wavefunction, $|\psi_0\rangle$,

$$|\psi_0\rangle = \frac{1}{\sqrt{2}} \left(|\phi^{*p}_{\ h}\rangle + |\phi^{*\bar{p}}_{\ \bar{h}}\rangle \right) . \tag{6}$$

Here any index with a bar denotes the opposite electron spin as compared to the index without a bar, and h and p are the special paired indices which correspond to the orbital that is primarily excited out of in the occupied space and the orbital that is primarily excited into for a particular excited state. Because these orbitals are so important for describing the excited state of interest, we will henceforth refer to them as the hole orbitals and the particle orbitals respectively. It is worth pointing out that our truncated ESMF reference, $|\psi_0\rangle$, bears many similarities to the reference in TD-CC,[75–77] as both wavefunctions represent the simplest possible state capable of describing open shell singlet excited states. As we will explain presently, however, our formulation differs significantly from TD-CC due to its "little t" structure and its projection-like operator.

Following the general strategy of CCSDt[87,88] but using the ESMF TOP orbital basis, we apply $\exp(\hat{T})$ to the Aufbau determinant, $|\phi_0^*\rangle$, which will serve as our "formal reference". Through a pseudoprojector and a careful initialization of our $\hat{T}$ operator, our formalism transforms the closed-shell, single-determinant $|\phi_0^*\rangle$ formal reference into the truncated ESMF reference $|\psi_0\rangle$ in a way that avoids many of the challenges typically associated with a multi-determinant reference. Of course, applying the exponential ansatz directly to the Aufbau determinant creates an immediate issue for excited states. Looking at the Taylor expansion of the exponential ansatz in equation 1, we see that the wavefunction would have a large contribution from the Aufbau determinant regardless of our initialization of $\hat{T}$, which is neither typical in excited states nor present in our desired ESMF reference. We address this issue by introducing a pseudoprojection operator $\hat{P}$ into the definition of our excited state pseudoprojected coupled-cluster (ESPCC) wavefunction.

$$|\Psi\rangle = \hat{P} e^{\hat{T}} \, |\phi_0^*\rangle \tag{7}$$

$$\hat{P} = 2 - \hat{a}_h^\dagger \hat{a}_h - \hat{a}_{\bar{h}}^\dagger \hat{a}_{\bar{h}} \tag{8}$$

Here $\hat{a}_h^\dagger / \hat{a}_{\bar{h}}^\dagger$ and $\hat{a}_h / \hat{a}_{\bar{h}}$ are the creation and destruction operators for the hole orbitals that are excited out of in the ESMF reference, and the 2 comes from the total number of these orbitals (one alpha and one beta). $\hat{P}$ deletes determinants in which the hole orbital is doubly occupied, and so in particular deletes the Aufbau determinant.

Like a true projector, the pseudoprojector $\hat{P}$ deletes certain pieces of the wavefunction like the Aufbau determinant, but, unlike a true projector, it modifies the coefficients on some of the pieces that are not deleted. Note that we avoid using the seemingly more straightforward true projector $\hat{P}_A = 1 - |\phi_0^*\rangle \langle \phi_0^*|$ whose only effect is to delete the Aufbau contribution, because it breaks size intensivity. As discussed in Section II F below, the pseudoprojector in equation 8 maintains both size extensivity and size intensivity. We also note that by deviating slightly from a rigid value of 2 in equation 8, we could introduce the flexibility to allow some Aufbau contribution, which does occur for excited states in the same symmetry representation as the ground state. One could also consider multi-orbital generalizations of $\hat{P}$ that could work with a less truncated ESMF reference, but for simplic-

ity in this initial study we stick to the pseudoprojector in equation 8. It's worth emphasizing that the details of the hole orbitals in the pseudoprojection operator are completely specified by the ESMF procedure. To help organize the wavefunctions presented so far, we have compiled them in Table 1.

C. The Cluster Operator

As is the case in other single-reference-based CC methods aimed at strongly multireference situations,[87–90] a choice must be made as to which excitation operators are included in the wavefunction. In order to produce an analog to ground state CCSD, we wish to include the excitations necessary to produce all determinants that are a single or double excitation away from the truncated ESMF reference, as illustrated in Figure 1. To do so, we require a subset of triple excitations relative to the Aufbau determinant, which leads to the following form for our cluster operator,

$$\hat{T} = \hat{T}_1 + \hat{T}_2 + \hat{T}_{\bar{3}}, \tag{9}$$

where $\hat{T}_{\bar{3}}$ represents only a small subset of all possible triples, specifically those which include a hole-particle TOP. Note that, despite the fact that not all double excitations off the Aufbau determinant, $|\phi_0^*\rangle$, are within the first order interacting space of our reference, $|\psi_0\rangle$, all of the double excitation operators must be included in order to ensure size intensivity, as will be illustrated in Section II F. As stated above, we will initialize our CC ansatz such that it reconstructs the truncated ESMF wavefunction in equation 6. By writing the relevant ESMF CI coefficients in CC form, i.e. by setting $t_{\bar{h}}^{p} = t_{\bar{h}}^{\bar{p}} = \frac{1}{\sqrt{2}}$ and $t_{\bar{h}\bar{h}}^{p\bar{p}} = -\frac{1}{2}$, we can exactly reconstruct the truncated ESMF state as the initial guess for our CC wavefunction $|\Psi\rangle$.

The introduction of the pseudoprojector in equation 7 adds an extra layer of complexity that is not present in the ground state theory. In the Taylor series expansion of our wavefunction, components of $\hat{T}$ that contain a hole index survive the pseudoprojector and appear at linear order, whereas the linear order appearances of components without the special hole index are eliminated by the pseudoprojector. Thus, these components only contribute to $|\Psi\rangle$ via $\hat{T}^2$ or higher order terms in which they appear alongside a component with the special hole index. We expect that $t_{\bar{h}}^{p}$ and $t_{\bar{h}}^{\bar{p}}$ will be the largest components of $\hat{T}_1$, so the largest contributions from excitation operators that do not contain a hole index will appear inside $\hat{T}^2$, where they will show up in cross terms with $t_{\bar{h}}^{p}$ and $t_{\bar{h}}^{\bar{p}}$. So, for a cluster amplitude such as t_{jk}^{bc} that contains no hole index, the primary contribution will be to the part of Hilbert space projected to by $\langle \phi^{*}{}_{hjk}^{pbc}|$ and $\langle \phi^{*}{}_{\bar{h}jk}^{\bar{p}bc}|$. In stark contrast to ground state CCSD, the projection of Hilbert space usually associated with this amplitude, $\langle \phi^{*}{}_{jk}^{bc}|$, is actually relatively unimportant, as it is more than two excitations away from the truncated ESMF reference. In the amplitude equations below, we will project with $\langle \phi^{*}{}_{hjk}^{pbc}| + \langle \phi^{*}{}_{\bar{h}jk}^{\bar{p}bc}|$ and then ensure that the corresponding projection, $\langle \phi^{*}{}_{hjk}^{pbc}| - \langle \phi^{*}{}_{\bar{h}jk}^{\bar{p}bc}|$, is satisfied by enforcing $t_{hjk}^{pbc} = -t_{\bar{h}jk}^{\bar{p}bc}$, which has the added benefit of avoiding any potential redundancy in the amplitudes. It is worth noting that, unlike the sufficiency conditions often introduced in Jeziorski-Monkhort based MRCC methods, the amplitude equations resulting from this system of linear combinations of projections are uniquely satisfied when the individual projections are satisfied, and thus satisfy the proper residual problem.[62–64] Furthermore, while it might be tempting to instead simply remove any parts of $\hat{T}$ that only contribute through $\hat{T}^2$ and higher terms, these components are critically important for maintaining size intensivity, as will be detailed in Section 2.6.

Lastly, we set the theory's definition of intermediate normalization by fixing at $\frac{1}{\sqrt{2}}$ the $t_{\bar{h}}^{p}$ and $t_{\bar{h}}^{\bar{p}}$ amplitudes used to construct the truncated ESMF reference. This is analogous to how the Aufbau coefficient is always 1 in the expanded CCSD wavefunction. Here, our choice of intermediate normalization ensures a unique solution to the forthcoming amplitude equations and also creates the following parallel to the ground state theory,

$$\langle \psi_0 | \Psi \rangle = \langle \psi_0 | \, \hat{P} e^{\hat{T}} \, | \phi_0^* \rangle = 1, \tag{10}$$

which matches the CCSD expression,

$$\langle \phi_0 | \psi_{CCSD} \rangle = \langle \phi_0 | \, e^{\hat{T}} \, | \phi_0 \rangle = 1. \tag{11}$$

D. The Energy and Amplitude Equations

With an excited-state-appropriate CC wavefunction to get us started, we now invoke the usual CC procedure to produce an approximate, non-variational energy equation as well as a set of amplitude equations. To obtain the energy equation, we project against the truncated ESMF reference, $|\psi_0\rangle$:

$$E \equiv \frac{\langle \psi_0 | \, e^{-\hat{T}} \hat{H} \, | \Psi \rangle}{\langle \psi_0 | \, e^{-\hat{T}} \, | \Psi \rangle} = \frac{\langle \psi_0 | \, e^{-\hat{T}} \hat{H} \hat{P} e^{\hat{T}} \, | \phi_0^* \rangle}{\langle \psi_0 | \, e^{-\hat{T}} \hat{P} e^{\hat{T}} \, | \phi_0^* \rangle}. \tag{12}$$

With the intermediate normalization introduced in the previous section, the denominator in this expression evaluates to 1. Similarly, the amplitude equations are defined by taking projections against all possible excited determinants no more than two excitations from the truncated ESMF reference, as are illustrated in Figure 1:

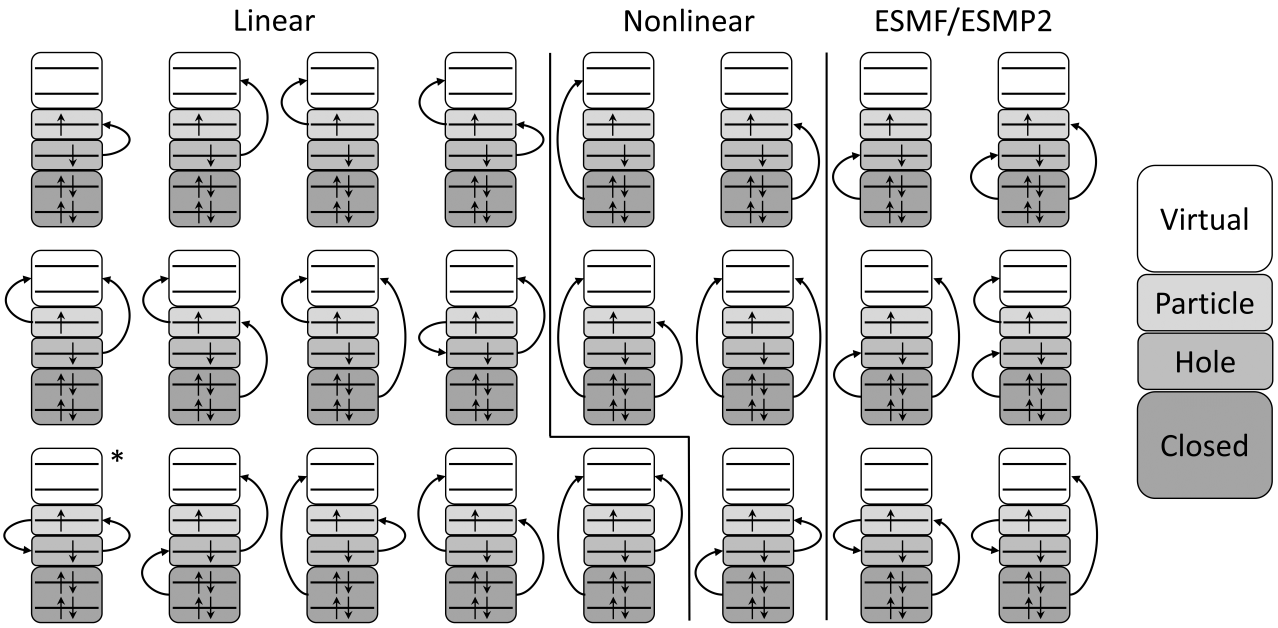

Figure 1. Presented here are all determinants within two excitations of one of the two determinants comprising the truncated ESMF reference. Note that the Aufbau determinant is intentionally missing, as it is removed by our pseudoprojector. The orbital space can be divided into four distinct regions: the closed space, hole space, particle space, and virtual space. The closed and hole spaces together form the set of orbitals which are occupied in the Aufbau determinant, while the particle and virtual spaces combine to form the set of unoccupied orbitals for the Aufbau determinant. Furthermore, the hole and particle TOP orbitals comprise the set of orbitals which are primarily excited out of and into respectively for the excited state of interest and are determined by an SVD of the original ESMF starting point. The entire set of determinants is also partitioned according to where they appear in the current theory. Those determinants under the linear heading either contain a hole in the hole space but not a TOP or contain multiple holes in the hole space, and thus are treated primarily by excitation operators appearing at linear order in the Taylor expansion of the exponential ansatz. In contrast, those under the nonlinear heading contain a single TOP with no additional holes in the hole space, and therefore see large contributions from the quadratic order $\hat{T}^2$ terms. Finally, those under the ESMF/ESMP2 heading are missed in the current implementation because they contain completely filled hole orbitals and thus are destroyed by our pseudoprojector, though their contribution is later estimated and corrected for via both the ESMF and ESMP2 theories. The determinant marked by an '*' corresponds to the spin flipped TOP, which while included in the theory has its amplitude fixed to achieve intermediate normalization.

$$\langle \phi^{*a}_{i} | \, e^{-\hat{T}} \left(\hat{H} - E \right) \hat{P} e^{\hat{T}} \, | \phi^{*}_{0} \rangle = 0, \tag{13}$$

$$\langle \phi^{*ab}_{ij} | \, e^{-\hat{T}} \left(\hat{H} - E \right) \hat{P} e^{\hat{T}} \, | \phi^{*}_{0} \rangle = 0, \tag{14}$$

$$\langle \phi^{*pbc}_{hjk} | \, e^{-\hat{T}} \left(\hat{H} - E \right) \hat{P} e^{\hat{T}} \, | \phi^{*}_{0} \rangle = 0. \tag{15}$$

Note that we do not have amplitude equations for all singles, doubles, and especially triples, only those in the "linear" and "nonlinear" categories in Figure 1. While satisfying the remaining singles and doubles amplitude equations under the "ESMF/ESMP2" category of Figure 1 would make for an ideal parallel to ground state CCSD, with the simple pseudoprojector scheme that we use here, our wavefunction does not have the flexibility to access these regions of Hilbert space, although we anticipate that more general choices of the pseudoprojector may resolve this issue in the future. For now, the energetic contributions of these missing terms will be estimated and corrected for by taking the corresponding terms' energy contributions from untruncated ESMF and ESMP2. Finally, with all singles and doubles present in $\hat{T}$ despite the fact that we only include singles and doubles bra states within two excitations of our truncated ESMF reference in equations 13 and 14, it may seem at first glance that we have a mismatch between the number of amplitudes and amplitude equations. However, as will be illustrated in the following section, the seemingly extra singles and doubles amplitudes go along with the single-TOP-containing doubles and triples amplitude equations, respectively, leaving us with the exact same number of amplitude equations as we have amplitudes to solve for.

E. Solving the Amplitude Equations

As mentioned in Section 2.3, there exist two distinct groups of excitation operators: those which contain a hole orbital as one of their indices and those that do not.

Those which do survive the pseudoprojection operator and contribute at linear order in the Taylor expansion of the wavefunction, while those which do not are destroyed by the pseudoprojector and therefore first appear at quadratic order where they must be paired with an excitation that does contain a hole index. As a result, we find it effective to use different approaches for these two distinct classes of amplitudes in the iterative solution of the amplitude equations.

To solve the amplitude equations, we make use of a quasi-Newton iterative scheme reminiscent of that often used in ground state CC.[97] To calculate the approximate Jacobian, we begin by approximating the Hamiltonian as only the diagonal portion of the Fock operator constructed from the ESMF density matrix. It is worth noting that during the ESMF optimization the orbitals were rotated such that they are no longer in a canonical regime.[58–60] However, we expect that the Fock matrix should remain mostly diagonally dominant, so we ignore the off-diagonal terms. While this approximation was successful for achieving tight convergence in the states tested within this paper, it is worth noting that more robust optimization algorithms whose approximate Jacobians includes off diagonal elements are possible. In the present algorithm, for a given cluster amplitude t_μ containing either a hole index without a TOP or multiple hole indices, we obtain a diagonal approximate Jacobian which leads to an update scheme very similar to that in the ground state theory:

$$t_\mu^{new} = t_\mu^{old} - \frac{\langle \phi_\mu^* | \, e^{-\hat{T}} (\hat{H} - E) e^{\hat{T}} \, | \phi_0^* \rangle}{N_\mu \left(\Delta_\mu + (E - E_0) \right)}. \tag{16}$$

Here $\langle \phi_\mu^* |$ corresponds to the Hilbert subspace resulting from the action of $\hat{T}_\mu$ on $|\phi_0^*\rangle$, Δ_μ is the orbital energy difference (using the diagonal elements of our Fock operator) corresponding to the $\hat{T}_\mu$ excitation, N_μ is the number of hole indices in the cluster amplitude, and $E_0 = \langle \phi_0^* | \, \hat{H} \, | \phi_0^* \rangle$.

For the cluster amplitudes that lack a hole index, the update is a little less conventional and is paired with the update for the related one-higher-excitation amplitude that contains the hole-particle TOP. As discussed in Section II C, the most important contribution from a no-hole cluster amplitude t_ν occurs in the terms inside $\hat{T}^2$ in which it partners with t_h^p or $t_{\bar{h}}^{\bar{p}}$ in an overall excitation that is one higher than t_ν itself. Thus, we update t_ν in conjunction with the amplitudes t_ω and $t_{\bar{\omega}}$, which are like t_ν but contain an additional TOP excitation. For example, if t_ν is t_{jk}^{bc}, then t_ω is t_{hjk}^{pbc} and $t_{\bar{\omega}}$ is $t_{\bar{h}ij}^{\bar{p}ab}$.

$$t_\nu^{new} = t_\nu^{old} - \frac{\left(\langle \phi_\omega^* | + \langle \phi_{\bar{\omega}}^* | \right) e^{-\hat{T}} (\hat{H} - E) e^{\hat{T}} \, | \phi_0^* \rangle}{(t_h^p + t_{\bar{h}}^{\bar{p}}) \Delta_\nu}, \tag{17}$$

$$t_\omega^{new} = t_\omega^{old} - \frac{\left(\langle \phi_\omega^* | - \langle \phi_{\bar{\omega}}^* | \right) e^{-\hat{T}} (\hat{H} - E) e^{\hat{T}} \, | \phi_0^* \rangle}{2 \left(\Delta_\omega + (E - E_0) \right)}, \tag{18}$$

$$t_{\bar{\omega}}^{new} = -t_\omega^{new} \tag{19}$$

Crucially, only two of these three amplitudes are independent variables ($t_{\bar{\omega}}$ being defined as the negative of t_ω as discussed in Section II C), which is why we are able to arrive at this style of iterative update from just two amplitude equations (the ones involving $\langle \phi_\omega^* |$ and $\langle \phi_{\bar{\omega}}^* |$) without encountering a linear dependency. Also note that, in our present formalism, t_h^p and $t_{\bar{h}}^{\bar{p}}$ are fixed at $1/\sqrt{2}$ by intermediate normalization.

In addition to the above approach to iterative amplitude updates, we choose to employ a two phase optimization procedure. While a two phase procedure is not strictly necessary, we find that it assists in achieving rapid and tight convergence of the residual equations. In the first phase, the two "higher order" excitation amplitudes t_ω and $t_{\bar{\omega}}$ are held fixed at zero, leaving only the amplitude associated with equation 17, t_ν, to change. After this subset of residual equations is sufficiently converged, the remaining amplitudes associated with equations 18 and 19 are introduced and all the residual equations are iterated until tight convergence is achieved. Finally, to accelerate the convergence of our method we utilize a DIIS implementation[100] which is turned on after the first few iterations, and whose history is reset when transitioning from phase I to phase II of the iterative scheme.

F. Size Extensivity and Size Intensivity

Size extensivity is a central property of coupled-cluster methods which guarantees that the correlation energy of the multi-electronic system scales linearly with system size in the large-system limit as it should. This property is ensured so long as the working equations contain no unlinked diagrams,[101,102] which is famously true of the ground state CC equations in equations 2-4, which contain only connected, and therefore linked, diagrams. While the introduction of the pseudoprojection operator in ESPCC complicates the equations, a diagrammatic analysis reveals that all unlinked diagrams cancel out, leaving only linked diagrams in the working equations. Therefore, ESPCC is a fully size extensive method, in parallel to its ground state counterpart.

Size intensivity, which ensures that a method's excitation energy on one molecule is unchanged by the addition of other noninteracting molecular fragments, is another important quality to achieve for an excited state method. Because ESPCC's excitation energies are energy differences against traditional ground state CCSD, achieving size intensive excitation energies requires that ESPCC's energy contributions from noninteracting molecular fragments that do not participate in the excitation must be exactly equal to those fragments' CCSD energies. To see that this is indeed the case, imagine that there are two noninteracting molecular fragments, one of which is in its excited state, molecular fragment A, and another which is in its ground state, molecular fragment B. Under these circumstances, our wavefunction maintains the

usual product factorizability due to the local nature of the pseudoprojector in equation 8 (indeed, $\hat{P}$, which we will write here as $\hat{P}_A$, only acts on A):

$$|\Psi\rangle = \hat{P}_A e^{\hat{T}_A+\hat{T}_B} |\phi_A^*\rangle \otimes |\phi_B\rangle = \left(\hat{P}_A e^{\hat{T}_A} |\phi_A^*\rangle\right) \otimes e^{\hat{T}_B} |\phi_B\rangle . \tag{20}$$

Note that this factorization would not work if we employed the intuitive, true projector $\hat{P} = 1 - |\phi_0^*\rangle \langle\phi_0^*|$, as it acts globally on both fragments A and B. Due to the product factorization shown in equation 20, the energy expression in equation 12 decomposes into

$$\begin{aligned} &\frac{\langle\psi_{0A}| e^{-\hat{T}_A} \hat{H}_A \hat{P}_A e^{\hat{T}_A} |\phi_A^*\rangle}{\langle\psi_{0A}| e^{-\hat{T}_A} \hat{P}_A e^{\hat{T}_A} |\phi_A^*\rangle} + \langle\phi_B| e^{-\hat{T}_B} \hat{H}_B e^{\hat{T}_B} |\phi_B\rangle \\ &= E_A + E_B \\ &= E, \end{aligned} \tag{21}$$

where the first term in this equation is the excited state energy for fragment A and the second term is the ground state energy expression for fragment B. This energy expression shows great promise of size intensivity, but in order to guarantee size intensivity in practice it must be shown that the iterative procedure produces the correct ground state amplitudes for fragment B, and thus the correct ground state CCSD energy expression for fragment B. It can be shown that in a noninteracting regime where the i, h, a, p indices in the projection belong to fragment A and the remaining j, k, b, c indices belong to fragment B, equations 14 and 15 factorize to produce

$$t_i^a \langle\phi_{B\,j}^{\;b}| e^{-\hat{T}_B} \hat{H}_B e^{\hat{T}_B} |\phi_B\rangle = 0, \tag{22}$$

$$t_h^p \langle\phi_{B\,jk}^{\;bc}| e^{-\hat{T}_B} \hat{H}_B e^{\hat{T}_B} |\phi_B\rangle = 0. \tag{23}$$

Note that, for at least the cluster amplitudes which construct our truncated ESMF reference, $t_h^p/t_{\bar{h}}^{\bar{p}}$, the t_i^a amplitudes cannot be zero. Therefore, to satisfy these amplitude equations, the fragment B portion of the equations must be zero, which is exactly equivalent to the ground state CCSD amplitude equations 3 and 4 for fragment B. While this is sufficient for proving size intensivity, we can make an even stronger claim. By plugging these expressions into the phase I iterative method in equation 17, we find that the iterative update for cluster amplitudes on fragment B is given by

$$t_\nu^{new} = t_\nu^{old} - \frac{\langle\phi_{B\nu}| e^{-\hat{T}_B} \hat{H}_B e^{\hat{T}_B} |\phi_B\rangle}{\Delta_\nu}, \tag{24}$$

which is exactly equivalent to the traditional ground state CCSD iterative update. In other words, at any iteration during phase I of this method, the cluster amplitudes that are noninteracting with the excitation will be exactly equivalent to their counterparts in a ground state CCSD calculation (see Supporting Information for more details). We would likewise expect that amplitudes that interact only weakly with the excitation will behave very similarly as in CCSD, creating a strong connection between the ground and excited state theories.

III. RESULTS

A. Computational Details

To implement this theory, we first derived by hand the tensor contractions that would be necessary for the energy and amplitude equations if we were using a full $\hat{T}_3$ operator containing all triples. We then applied an automatic code generator to split each term involving triples into the various sub-terms corresponding to the $O(N^4)$ subset of the triples that are actually included in our $\hat{T}_{\tilde{3}}$. This guarantees an N^4 memory footprint, and, as discussed in the next section, leads to an implementation with an N^6 cost scaling.

For all of the forthcoming results, the EOM-CCSD and δ-CR-EOM-CC(2,3),D[103–109] calculations were performed with GAMESS,[110,111] while the CISD and FCI calculations were performed with PySCF.[112–114] To obtain the timing and scaling data, calculations were performed on a single core on the same machine to ensure consistency. No frozen core approximation was utilized on any of these methods. For our method, we iterate until the maximum amplitude equation residual was no larger than 10^{-10}, and for all other methods we utilize the default convergence settings. For the "ESMF/ESMP2" terms in Figure 1, we run an N^5-cost ESMP2 calculation,[61] extract the energy contribution for these terms, and add it to our CC energy to form our corrected ESPCC energy.

B. Scaling Analysis and Computational Cost

With the inclusion of a subset of triples amplitudes, one might begin to wonder whether the scaling of this method may be worse than its ground state counterpart. However, due to the transformation to the TOP orbital basis and the truncation of the ESMF wavefunction, we find that the asymptotic scaling remains equivalent to CCSD at $O(N^6)$. In order to verify this scaling, we collected a series of timing data in order to analyze the scaling contribution of each term in the current implementation. To collect this data, we timed the contribution from each term in the theory on a system of spatially separated, minimal basis H_2 molecules ranging from 5 to 25 molecules. The timing data for each term was then plotted on a log-log plot and fit to a least squares linear regression. The slope resulting from each regression was conservatively rounded up to the nearest whole number and binned according to scaling. These results are reported along with the minimum and mean coefficient of correlation for the linear regression, R, in Table 2. It is worth noting that the maximum slope for any regression was 5.829, thereby confirming our proposed $O(N^6)$ scaling. Furthermore, each of the linear regressions for the N^6 scaling terms was manually reviewed to ensure that the plots did indeed appear well fit by the regression.

	1	N	N^2	N^3	N^4	N^5	N^6
Number of terms	4	17953	7047	5622	3899	2381	293
Min R	-0.074	0.002	0.888	0.921	0.855	0.875	0.996
Mean R	-.056	0.878	0.977	0.988	0.990	0.993	0.999

Table 2. Asymptotic scaling analysis of all terms[a]

[a]Presented are the total number of terms belonging to each asymptotic scaling group along with the minimum and mean correlation coefficients for the linear regression, R. The high R values in combination with a manual review of the linear fits on the higher scaling terms confirms that the presented theory asymptotically scales at the same N^6 scaling as ground state CCSD.

For a number of the lower scaling terms, the coefficient of correlation indicates a lower quality for the linear regression. Because many of these terms have timings on the order of milliseconds, we suspect that a combination of the overhead for the matrix multiplication functions or the random variations in processor performance may be obfuscating the exact linear relationship. However, we have no reason to believe they would affect the method's asymptotic N^6 scaling. Note that, while some optimization in the form of tensor contraction ordering was done to ensure an $O(N^6)$ scaling, no other optimization was performed for this implementation. For example, we have not yet attempted any factorization of the amplitude equations nor have we consolidated the terms which are related through simple permutations of each other, and so the number of terms in Table 2 is unnecessarily large. With a more careful implementation, we suspect that a large reduction in the total number of terms and wall time will be possible.

At this point, it is worth noting that if one desires to find multiple excited states, for each excited state an independent ESMF starting point would need to be determined followed by an independent ESPCC calculation. While the need for a separate calculation for each different state is typical amongst state-specific CC methods, it does noticeably differ from methods such as EOM-CC which through their diagonalization of the similarity transformed Hamiltonian can determine multiple states simultaneously.

C. Small basis testing

For the initial evaluation of ESPCC, we studied its performance on H_6 (Table 3) and H_2O (Table 4) in a 6-31G basis. With these small molecules in a small basis, we are able to compare the errors of this method directly with FCI. The excitation energy errors with respect to FCI are reported in Figure 2. For H_6, we have one H_2 in the center with a slightly stretched bond surrounded by two other H_2 with equilibrium bond lengths approximately 3Å away. We see that EOM-CCSD and ESPCC both with and without the ESMP2-based correction almost perfectly match both the absolute and excitation FCI energies, while ESMF and ESMP2 have a little more difficulty, presumably due to their less complete correlation treatments.

For H_2O, our method and EOM-CCSD perform comparably for absolute energies, but the sign of the error is very important. The ground state CCSD calculation errors high for the ground state energy, so EOM-CCSD erring low for the excited state energy causes it to perform worse than ESMP2 and both the uncorrected and corrected versions of ESPCC for the excitation energy. This cancellation of errors is important when determining excitation energies, and results in our method performing almost an order of magnitude better than EOM-CCSD in this case. Although further study is needed, it would make sense if the present theory, in which ground and excited state are treated on a much more equal footing, had better error cancellation tendencies.

D. Larger basis testing

With promising results in our initial assessment, we now test these methods in the slightly larger cc-pVDZ basis on the excited states of H_2O (Table 4), formaldehyde (CH_2O) (Table 5), ketene (CH_2CO) (Table 6), and ammonia difluorine (NH_3 F_2) (Table 7). Of these excitations, the ammonia difluorine charge transfer excitation is especially noteworthy as state-specific orbital relaxations should be particularly important. Finally, we also test these methods on neon (Table 8) in an aug-cc-pVTZ basis in order to investigate performance in a Rydberg excitation. Because both the molecule size and basis size have grown, using FCI as a reference is no longer convenient. Therefore, we have used the triples corrected, N^7 scaling CR-CC(2,3) and δ-CR-EOM-CC(2,3),D as our new ground and excited references respectively. The excitation energies errors with respect to δ-CR-EOM-CC(2,3),D are reported in Figure 2.

In these larger basis sets especially, it is evident that the inclusion of the ESMP2-based correction is critical for maintaining a competitive accuracy for ESPCC. As a result, future work should explore the development of versions of ESPCC which do not need to rely on an ESMP2 correction for missing terms. For now, the ESMP2-based correction provides a reasonable estimate of the influence of these terms, and thus the ESMP2-corrected ESPCC will be the primary focus of the following comparisons with other methods.

For H_2O, EOM-CCSD has both a better absolute and excitation energy as compared to ESPCC. However, in formaldehyde we see the opposite trend, with ESPCC

Method	Energy (Ha)		Excitation
	Ground	Excited	Energy (eV)
FCI	−3.437 120	−2.935 923	13.6383
ESMF	−3.356 782	−2.880 453	12.9616
ESMP2	−3.411 371	−2.919 699	13.3791
ESPCC	−3.437 119	−2.935 919	13.6386
Corrected ESPCC	−3.437 119	−2.935 919	13.6383
EOM-CCSD	−3.437 119	−2.935 910	13.6386

Table 3. H_6 ground, excited, and vertical excitation energies in the 6-31G basis.

	6-31G Basis			cc-pVDZ Basis		
Method	Energy (Ha)		Excitation	Energy (Ha)		Excitation
	Ground	Excited	Energy (eV)	Ground	Excited	Energy (eV)
FCI	−76.120 137	−75.803 955	8.604	—	—	—
δ-CR-EOM-CC(2,3),D	—	—	—	−76.242 856	−75.937 963	8.297
ESMF	−75.984 322	−75.692 508	7.941	−76.027 022	−75.747 005	7.620
ESMP2	−76.112 169	−75.794 302	8.650	−76.230 220	−75.923 046	8.359
ESPCC	−76.118 633	−75.801 109	8.641	−76.239 548	−75.923 188	8.609
Corrected ESPCC	−76.118 633	−75.801 860	8.621	−76.239 548	−75.932 350	8.359
EOM-CCSD	−76.118 633	−75.806 267	8.501	−76.239 548	−75.935 170	8.283

Table 4. Water (H_2O) ground, excited, and vertical excitation energies in the 6-31G and cc-pVDZ bases.

Method	Energy (Ha)		Excitation
	Ground	Excited	Energy (eV)
δ-CR-EOM-CC(2,3),D	−114.221 280	−114.071 520	4.075
ESMF	−113.877 084	−113.752 709	3.384
ESMP2	−114.195 345	−114.040 002	4.227
ESPCC	−114.211 046	−114.034 620	4.801
Corrected ESPCC	−114.211 046	−114.056 952	4.193
EOM-CCSD	−114.211 046	−114.054 292	4.266

Table 5. Formaldehyde (CH_2O) ground, excited, and vertical excitation energies in the cc-pVDZ basis.

Method	Energy (Ha)		Excitation
	Ground	Excited	Energy (eV)
δ-CR-EOM-CC(2,3),D	−152.214 501	−152.075 519	3.782
ESMF	−151.740 890	−151.610 512	3.548
ESMP2	−152.181 539	−152.042 782	3.776
ESPCC	−152.196 705	−152.031 461	4.497
Corrected ESPCC	−152.196 705	−152.057 364	3.792
EOM-CCSD	−152.196 705	−152.044 487	4.142

Table 6. Ketene (CH_2CO) ground, excited, and vertical excitation energies in the cc-pVDZ basis.

Method	Energy (Ha)		Excitation
	Ground	Excited	Energy (eV)
δ-CR-EOM-CC(2,3),D	−255.507 183	−255.166 706	9.265
ESMF	−254.879 868	−254.593 956	7.780
ESMP2	−255.468 537	−255.137 512	9.008
ESPCC	−255.493 049	−255.139 057	9.633
Corrected ESPCC	−255.493 049	−255.146 565	9.428
EOM-CCSD	−255.493 049	−255.133 689	9.779

Table 7. Ammonia difluorine (NH_3 F_2) ground, excited, and vertical excitation energies in the cc-pVDZ basis.

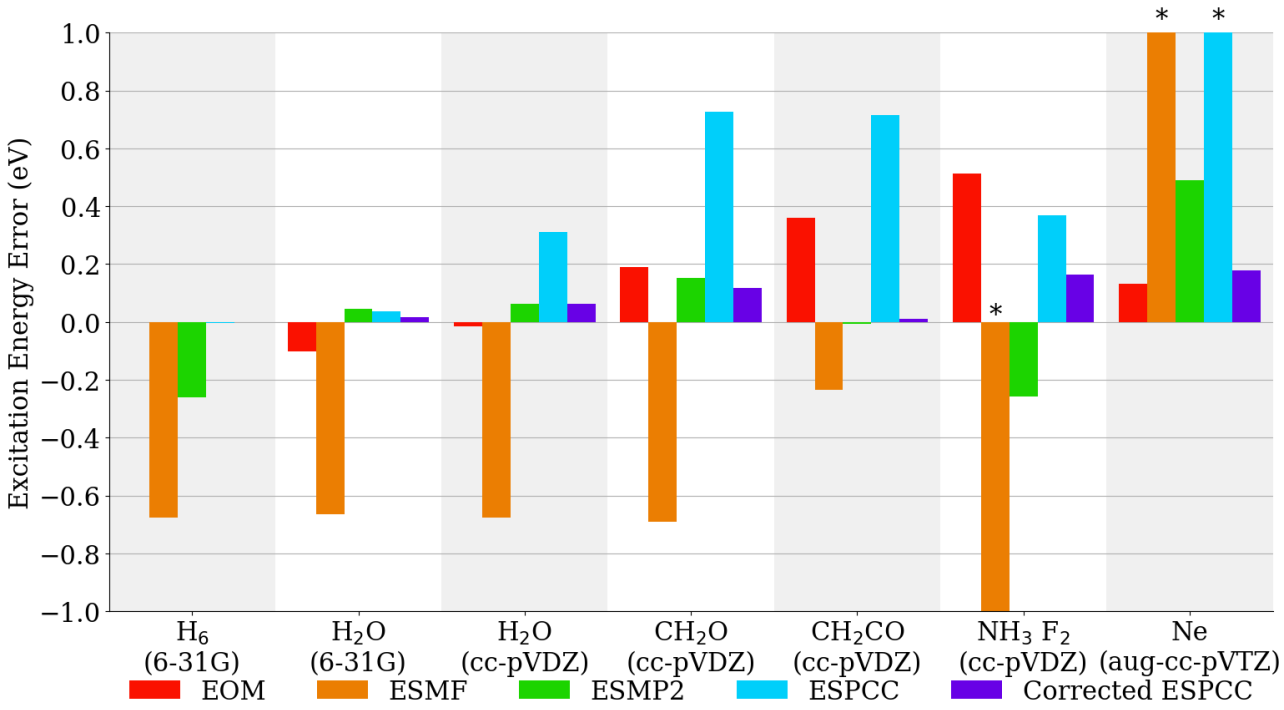

Figure 2. The excitation energy errors for (from left to right) EOM-CCSD, ESMF, ESMP2, ESPCC, and Corrected ESPCC on a small set of test molecules. For the two leftmost molecules in the smallest basis, the reference energy was determined via FCI, while for all remaining molecules the reference energy was calculated via δ-CR-EOM-CC(2,3),D. Bars marked with an '*' extend beyond the limits of the plot, precise numbers can be found in the tables above.

Method	Energy (Ha)		Excitation
	Ground	Excited	Energy (eV)
δ-CR-EOM-CC(2,3),D	−128.825 887	−127.094 052	47.126
ESMF	−128.533 273	−126.754 857	48.393
ESMP2	−128.819 179	−127.069 362	47.615
ESPCC	−128.820 401	−127.015 682	49.109
Corrected ESPCC	−128.820 401	−127.082 043	47.303
EOM-CCSD	−128.820 401	−127.083 667	47.259

Table 8. Neon (Ne) ground, excited, and vertical excitation energies in the aug-cc-pVTZ basis.

He atoms	ESMF	ESMP2	ESPCC	Corrected ESPCC	EOM-CCSD	CISD
0	7.620	8.359	8.609	8.359	8.283	11.600
1	7.620	8.359	8.609	8.359	8.283	12.404
2	7.620	8.359	8.609	8.359	8.283	13.198
3	7.620	8.359	8.609	8.359	8.283	13.983
4	7.620	8.359	8.609	8.359	8.283	14.760
5	7.620	8.359	8.609	8.359	8.283	15.528

Table 9. Excitation energies (eV) across multiple methods for cc-pVDZ water in the presence of a variable number of noninteracting He atoms[a]

[a]These results corroborate the proof of size intensivity presented earlier for this method, as well as illustrate how large of an influence a lack of size intensivity like that in CISD has on the quality of excitation energies.

slightly better than EOM-CCSD for both the absolute and excitation energies. For ketene, we observe the largest discrepancy, where our method results in a significantly lower absolute energy than EOM-CCSD which results in an error just under a hundredth of an eV for ESPCC versus an error on the order of tenths of eV for EOM-CCSD.

In the ammonia difluorine system, we study the lowest lying charge transfer which is from the ammonia lone pair to the difluorine. While methods such as EOM-CCSD have the ability to partially relax the orbitals after an excitation, in situations like this one where the charge density shifts dramatically, this partial relaxation may not be enough and can result in significant errors. In contrast, ESPCC builds a CC ansatz atop an already orbital relaxed, excited-state-specific starting point. This contrast manifests itself in our results, where ESPCC achieves a better absolute energy than EOM-CCSD which results in an excited state energy error a third that of EOM-CCSD.

Finally, we compare these methods in the 2s to 3p Rydberg excitation of Ne. While we may expect EOM-CCSD to face similar difficulties here as in charge transfer, it performs slightly better than ESPCC. It is worth noting that in this particular excited state, the size of the ESMP2 based correction is much larger than any previous molecule ($\sim$2 eV). It is possible that the error associated with the ESMP2 based correction may be responsible for the bulk of ESPCC's error here.

E. Size Intensive Energies

To test whether this method is size intensive as we expect, we calculate the excitation energy of H_2O in the presence of a variable number of very well separated He atoms. The results for these calculations on a variety of methods are shown in Table 9. As we can see, most of the methods presented produce the exact same excitation energy regardless of the number of noninteracting He atoms that are introduced. The exception is CISD, which has well known size consistency, and consequently size intensivity, issues. Because the ground state energy for ESPCC is calculated using traditional CCSD, the size intensivity of ESPCC implies that our method is correctly reproducing the CCSD ground state energy for the additional He atoms. Though one may begin to wonder whether the ESMP2 based correction affects the size intensivity of our method in any way, it is worth noting that this correction involves orbitals localized only on the fragment that is being excited, and thus does not affect the energy on any other fragment.

IV. CONCLUSION

We have presented an approach to excited-state-specific coupled-cluster theory that applies a simple pseudoprojector to a single-reference coupled-cluster expansion containing singles, doubles, and some triples in order to build a CCSD-like wavefunction atop an excited state mean field starting point. Like its ground state cousin, this ESPCC approach is size extensive, size intensive, has an N^6 cost, and can be optimized by a DIIS-accelerated diagonal Jacobian approximation. For amplitudes that do not interact with the excitation, the working equations simplify to match those of CCSD, while amplitudes that are only weakly coupled to the excitation see slightly modified CCSD-like working equations. With a correction from excited-state-specific perturbation theory to account for correlation terms incompatible with the simple pseudoprojector used in this initial exploration of ESPCC, excitation energies are within 0.2 eV of high-level benchmarks in tests that include valence states, a Rydberg state, and a charge transfer state. This compares favorably with the performance of ESMP2 and EOM-CCSD on the same states.

In the future, it will be especially interesting to explore more general forms for the pseudoprojection operator in order to both eliminate the reliance on perturbation theory corrections and admit a more full-fledged ESMF reference. Given that many of the doubles amplitudes experience working equations that are little different than those in CCSD, it will also be interesting to explore whether, at least for these amplitudes, straightforward analogues to ground state perturbative triples corrections can be formulated. Furthermore, it will be interesting to evaluate the performance of ESPCC on states involving large doubly excited character, and evaluating whether an augmentation of the cluster operator with selective quadruple excitations will be important for maintaining accuracy. Finally, a reimplementation in spatial rather than spin orbitals that exploits factorization and permutation symmetry should allow the theory to be tested on a much wider range of molecules and excited states.

V. ACKNOWLEDGEMENTS

This work was supported by the National Science Foundation's CAREER program under Award Number 1848012. Calculations were performed using the Berkeley Research Computing Savio cluster. H.T. acknowledges that this material is based upon work supported by the National Science Foundation Graduate Research Fellowship Program under Grant No. DGE 2146752. Any opinions, findings, and conclusions or recommendations expressed in this material are those of the authors and do not necessarily reflect the views of the National Science Foundation.

VI. REFERENCES

[1] Szabo, A.; Ostlund, N. S. *Modern quantum chemistry: introduction to advanced electronic structure theory*; Courier Corpo-

ration: New York, 2012.
[2]Møller, C.; Plesset, M. S. Note on an approximation treatment for many-electron systems. *Physical Review* **1934**, *46*, 618.
[3]Čížek, J. On the correlation problem in atomic and molecular systems. Calculation of wavefunction components in Ursell-type expansion using quantum-field theoretical methods. *The Journal of Chemical Physics* **1966**, *45*, 4256–4266.
[4]Čížek, J.; Paldus, J. Correlation problems in atomic and molecular systems III. Rederivation of the coupled-pair many-electron theory using the traditional quantum chemical methodst. *International Journal of Quantum Chemistry* **1971**, *5*, 359–379.
[5]Bartlett, R. J.; Musiał, M. Coupled-cluster theory in quantum chemistry. *Reviews of Modern Physics* **2007**, *79*, 291.
[6]Raghavachari, K.; Trucks, G. W.; Pople, J. A.; Head-Gordon, M. A fifth-order perturbation comparison of electron correlation theories. *Chemical Physics Letters* **1989**, *157*, 479–483.
[7]Watts, J. D.; Gauss, J.; Bartlett, R. J. Coupled-cluster methods with noniterative triple excitations for restricted open-shell Hartree–Fock and other general single determinant reference functions. Energies and analytical gradients. *The Journal of Chemical Physics* **1993**, *98*, 8718–8733.
[8]Thomas, J. R.; DeLeeuw, B. J.; Vacek, G.; Crawford, T. D.; Yamaguchi, Y.; Schaefer III, H. F. The balance between theoretical method and basis set quality: A systematic study of equilibrium geometries, dipole moments, harmonic vibrational frequencies, and infrared intensities. *The Journal of Chemical Physics* **1993**, *99*, 403–416.
[9]Helgaker, T.; Gauss, J.; Jørgensen, P.; Olsen, J. The prediction of molecular equilibrium structures by the standard electronic wave functions. *The Journal of Chemical Physics* **1997**, *106*, 6430–6440.
[10]Bak, K. L.; Gauss, J.; Jørgensen, P.; Olsen, J.; Helgaker, T.; Stanton, J. F. The accurate determination of molecular equilibrium structures. *The Journal of Chemical Physics* **2001**, *114*, 6548–6556.
[11]Hohenberg, P.; Kohn, W. Inhomogeneous electron gas. *Physical Review* **1964**, *136*, B864.
[12]Kohn, W.; Sham, L. J. Self-consistent equations including exchange and correlation effects. *Physical Review* **1965**, *140*, A1133.
[13]Parr, R. G. Density functional theory of atoms and molecules. Horizons of Quantum Chemistry: Proceedings of the Third International Congress of Quantum Chemistry Held at Kyoto, Japan, October 29-November 3, 1979. 1980; pp 5–15.
[14]Piela, L. *Ideas of quantum chemistry*; Elsevier: Amsterdam, 2013.
[15]Runge, E.; Gross, E. K. Density-functional theory for time-dependent systems. *Physical Review Letters* **1984**, *52*, 997.
[16]Burke, K.; Werschnik, J.; Gross, E. Time-dependent density functional theory: Past, present, and future. *The Journal of Chemical Physics* **2005**, *123*, 062206.
[17]Casida, M. E.; Huix-Rotllant, M. Progress in time-dependent density-functional theory. *Annual Review of Physical Chemistry* **2012**, *63*, 287–323.
[18]Monkhorst, H. J. Calculation of properties with the coupled-cluster method. *International Journal of Quantum Chemistry* **1977**, *12*, 421–432.
[19]Koch, H.; Kobayashi, R.; Sanchez de Merás, A.; Jørgensen, P. Calculation of size-intensive transition moments from the coupled cluster singles and doubles linear response function. *The Journal of Chemical Physics* **1994**, *100*, 4393–4400.
[20]Rowe, D. Equations-of-motion method and the extended shell model. *Reviews of Modern Physics* **1968**, *40*, 153.
[21]Stanton, J. F.; Bartlett, R. J. The equation of motion coupled-cluster method. A systematic biorthogonal approach to molecular excitation energies, transition probabilities, and excited state properties. *The Journal of Chemical Physics* **1993**, *98*, 7029–7039.
[22]Krylov, A. I. Equation-of-motion coupled-cluster methods for open-shell and electronically excited species: The hitchhiker's guide to Fock space. *Annual Review of Physical Chemistry* **2008**, *59*, 433–462.
[23]Caricato, M.; Trucks, G. W.; Frisch, M. J. On the difference between the transition properties calculated with linear response-and equation of motion-CCSD approaches. *The Journal of Chemical Physics* **2009**, *131*, 174104.
[24]Tozer, D. J.; Amos, R. D.; Handy, N. C.; Roos, B. O.; Serrano-Andres, L. Does density functional theory contribute to the understanding of excited states of unsaturated organic compounds? *Molecular Physics* **1999**, *97*, 859–868.
[25]Sobolewski, A. L.; Domcke, W. Ab initio study of the excited-state coupled electron–proton-transfer process in the 2-aminopyridine dimer. *Chemical Physics* **2003**, *294*, 73–83.
[26]Dreuw, A.; Weisman, J. L.; Head-Gordon, M. Long-range charge-transfer excited states in time-dependent density functional theory require non-local exchange. *The Journal of Chemical Physics* **2003**, *119*, 2943–2946.
[27]Dreuw, A.; Head-Gordon, M. Failure of time-dependent density functional theory for long-range charge-transfer excited states: the zincbacteriochlorin- bacteriochlorin and bacteriochlorophyll- spheroidene complexes. *Journal of the American Chemical Society* **2004**, *126*, 4007–4016.
[28]Mester, D.; Kállay, M. Charge-transfer excitations within density functional theory: how accurate are the most recommended approaches? *Journal of Chemical Theory and Computation* **2022**, *18*, 1646–1662.
[29]Izsák, R. Single-reference coupled cluster methods for computing excitation energies in large molecules: The efficiency and accuracy of approximations. *Wiley Interdisciplinary Reviews: Computational Molecular Science* **2020**, *10*, e1445.
[30]Kozma, B.; Tajti, A.; Demoulin, B.; Izsák, R.; Nooijen, M.; Szalay, P. G. A new benchmark set for excitation energy of charge transfer states: systematic investigation of coupled cluster type methods. *Journal of Chemical Theory and Computation* **2020**, *16*, 4213–4225.
[31]Tozer, D. J.; Handy, N. C. Improving virtual Kohn–Sham orbitals and eigenvalues: Application to excitation energies and static polarizabilities. *The Journal of Chemical Physics* **1998**, *109*, 10180–10189.
[32]Casida, M. E.; Jamorski, C.; Casida, K. C.; Salahub, D. R. Molecular excitation energies to high-lying bound states from time-dependent density-functional response theory: Characterization and correction of the time-dependent local density approximation ionization threshold. *The Journal of Chemical Physics* **1998**, *108*, 4439–4449.
[33]Casida, M. E.; Salahub, D. R. Asymptotic correction approach to improving approximate exchange–correlation potentials: Time-dependent density-functional theory calculations of molecular excitation spectra. *The Journal of Chemical Physics* **2000**, *113*, 8918–8935.
[34]Tozer, D. J.; Handy, N. C. The importance of the asymptotic exchange-correlation potential in density functional theory. *Molecular Physics* **2003**, *101*, 2669–2675.
[35]Tozer, D. J.; Handy, N. C. On the determination of excitation energies using density functional theory. *Physical Chemistry Chemical Physics* **2000**, *2*, 2117–2121.
[36]Maitra, N. T.; Zhang, F.; Cave, R. J.; Burke, K. Double excitations within time-dependent density functional theory linear response. *The Journal of Chemical Physics* **2004**, *120*, 5932–5937.
[37]Cave, R. J.; Zhang, F.; Maitra, N. T.; Burke, K. A dressed TDDFT treatment of the 21Ag states of butadiene and hexatriene. *Chemical Physics Letters* **2004**, *389*, 39–42.
[38]Levine, B. G.; Ko, C.; Quenneville, J.; MartÍnez, T. J. Conical intersections and double excitations in time-dependent density functional theory. *Molecular Physics* **2006**, *104*, 1039–1051.
[39]Tawada, Y.; Tsuneda, T.; Yanagisawa, S.; Yanai, T.; Hirao, K. A long-range-corrected time-dependent density functional theory. *The Journal of Chemical Physics* **2004**, *120*, 8425–8433.

[40]Yanai, T.; Tew, D. P.; Handy, N. C. A new hybrid exchange–correlation functional using the Coulomb-attenuating method (CAM-B3LYP). *Chemical Physics Letters* **2004**, *393*, 51–57.

[41]Musiał, M.; Bartlett, R. J. Charge-transfer separability and size-extensivity in the equation-of-motion coupled cluster method: EOM-CCx. *The Journal of Chemical Physics* **2011**, *134*, 034106.

[42]Ziegler, T.; Rauk, A.; Baerends, E. J. On the calculation of multiplet energies by the Hartree-Fock-Slater method. *Theoretica Chimica Acta* **1977**, *43*, 261–271.

[43]Kowalczyk, T.; Yost, S. R.; Voorhis, T. V. Assessment of the ΔSCF density functional theory approach for electronic excitations in organic dyes. *The Journal of Chemical Physics* **2011**, *134*, 054128.

[44]Gilbert, A. T.; Besley, N. A.; Gill, P. M. Self-consistent field calculations of excited states using the maximum overlap method (MOM). *The Journal of Physical Chemistry A* **2008**, *112*, 13164–13171.

[45]Besley, N. A.; Gilbert, A. T.; Gill, P. M. Self-consistent-field calculations of core excited states. *The Journal of Chemical Physics* **2009**, *130*, 124308.

[46]Barca, G. M.; Gilbert, A. T.; Gill, P. M. Simple models for difficult electronic excitations. *Journal of Chemical Theory and Computation* **2018**, *14*, 1501–1509.

[47]Kossoski, F.; Loos, P.-F. State-Specific Configuration Interaction for Excited States. *Journal of Chemical Theory and Computation* **2023**, *19*, 2258–2269.

[48]Mayhall, N. J.; Raghavachari, K. Multiple solutions to the single-reference CCSD equations for NiH. *Journal of Chemical Theory and Computation* **2010**, *6*, 2714–2720.

[49]Lee, J.; Small, D. W.; Head-Gordon, M. Excited states via coupled cluster theory without equation-of-motion methods: Seeking higher roots with application to doubly excited states and double core hole states. *The Journal of Chemical Physics* **2019**, *151*, 214103.

[50]Folkestad, S. D.; Sannes, B. S.; Koch, H. Entanglement coupled cluster theory: Exact spin-adaptation. *The Journal of Chemical Physics* **2023**, *158*, 224114.

[51]Kossoski, F.; Marie, A.; Scemama, A.; Caffarel, M.; Loos, P.-F. Excited States from State-Specific Orbital-Optimized Pair Coupled Cluster. *Journal of Chemical Theory and Computation* **2021**, *17*, 4756–4768.

[52]Marie, A.; Kossoski, F.; Loos, P.-F. Variational coupled cluster for ground and excited states. *The Journal of Chemical Physics* **2021**, *155*, 104105.

[53]Arias-Martinez, J. E.; Cunha, L. A.; Oosterbaan, K. J.; Lee, J.; Head-Gordon, M. Accurate core excitation and ionization energies from a state-specific coupled-cluster singles and doubles approach. *Physical Chemistry Chemical Physics* **2022**, *24*, 20728–20741.

[54]Rishi, V.; Ravi, M.; Perera, A.; Bartlett, R. J. Dark doubly excited states with modified coupled cluster models: A reliable compromise between cost and accuracy? *The Journal of Physical Chemistry A* **2023**, *127*, 828–834.

[55]Kowalczyk, T.; Tsuchimochi, T.; Chen, P.-T.; Top, L.; Van Voorhis, T. Excitation energies and Stokes shifts from a restricted open-shell Kohn-Sham approach. *The Journal of Chemical Physics* **2013**, *138*, 164101.

[56]Hait, D.; Head-Gordon, M. Excited state orbital optimization via minimizing the square of the gradient: General approach and application to singly and doubly excited states via density functional theory. *Journal of Chemical Theory and Computation* **2020**, *16*, 1699–1710.

[57]Hait, D.; Head-Gordon, M. Orbital optimized density functional theory for electronic excited states. *The Journal of Physical Chemistry Letters* **2021**, *12*, 4517–4529.

[58]Shea, J. A.; Neuscamman, E. Communication: A mean field platform for excited state quantum chemistry. *The Journal of Chemical Physics* **2018**, *149*, 081101.

[59]Shea, J. A.; Gwin, E.; Neuscamman, E. A generalized variational principle with applications to excited state mean field theory. *Journal of Chemical Theory and Computation* **2020**, *16*, 1526–1540.

[60]Hardikar, T. S.; Neuscamman, E. A self-consistent field formulation of excited state mean field theory. *The Journal of Chemical Physics* **2020**, *153*, 164108.

[61]Clune, R.; Shea, J. A.; Neuscamman, E. N5-scaling excited-state-specific perturbation theory. *Journal of Chemical Theory and Computation* **2020**, *16*, 6132–6141.

[62]Köhn, A.; Hanauer, M.; Mueck, L. A.; Jagau, T.-C.; Gauss, J. State-specific multireference coupled-cluster theory. *Wiley Interdisciplinary Reviews: Computational Molecular Science* **2013**, *3*, 176–197.

[63]Lischka, H.; Nachtigallova, D.; Aquino, A. J.; Szalay, P. G.; Plasser, F.; Machado, F. B.; Barbatti, M. Multireference approaches for excited states of molecules. *Chemical Reviews* **2018**, *118*, 7293–7361.

[64]Lyakh, D. I.; Musiał, M.; Lotrich, V. F.; Bartlett, R. J. Multireference nature of chemistry: The coupled-cluster view. *Chemical Reviews* **2012**, *112*, 182–243.

[65]Jeziorski, B.; Monkhorst, H. J. Coupled-cluster method for multideterminantal reference states. *Physical Review A* **1981**, *24*, 1668.

[66]Kucharski, S. A.; Bartlett, R. J. Hilbert space multireference coupled-cluster methods. I. The single and double excitation model. *The Journal of Chemical Physics* **1991**, *95*, 8227–8238.

[67]Piecuch, P.; Kowalski, K. The state-universal multi-reference coupled-cluster theory: An overview of some recent advances. *International Journal of Molecular Sciences* **2002**, *3*, 676–709.

[68]Hubač, I.; Neogrády, P. Size-consistent Brillouin-Wigner perturbation theory with an exponentially parametrized wave function: Brillouin-Wigner coupled-cluster theory. *Physical Review A* **1994**, *50*, 4558.

[69]Pittner, J.; Nachtigall, P.; Čársky, P.; Mášik, J.; Hubač, I. Assessment of the single-root multireference Brillouin–Wigner coupled-cluster method: Test calculations on CH 2, SiH 2, and twisted ethylene. *The Journal of Chemical Physics* **1999**, *110*, 10275–10282.

[70]Mahapatra, U. S.; Chattopadhyay, S. Potential energy surface studies via a single root multireference coupled cluster theory. *The Journal of Chemical Physics* **2010**, *133*, 074102.

[71]Mahapatra, U. S.; Chattopadhyay, S. Evaluation of the performance of single root multireference coupled cluster method for ground and excited states, and its application to geometry optimization. *The Journal of Chemical Physics* **2011**, *134*, 044113.

[72]Mahapatra, U. S.; Datta, B.; Mukherjee, D. A state-specific multi-reference coupled cluster formalism with molecular applications. *Molecular Physics* **1998**, *94*, 157–171.

[73]Mahapatra, U. S.; Datta, B.; Mukherjee, D. A size-consistent state-specific multireference coupled cluster theory: Formal developments and molecular applications. *The Journal of Chemical Physics* **1999**, *110*, 6171–6188.

[74]Hanrath, M. An exponential multireference wave-function Ansatz. *The Journal of Chemical Physics* **2005**, *123*, 084102.

[75]Balková, A.; Bartlett, R. J. Coupled-cluster method for open-shell singlet states. *Chemical Physics Letters* **1992**, *193*, 364–372.

[76]Szalay, P. G.; Bartlett, R. J. Analytic energy gradients for the two-determinant coupled cluster method with application to singlet excited states of butadiene and ozone. *The Journal of Chemical Physics* **1994**, *101*, 4936–4944.

[77]Lutz, J. J.; Nooijen, M.; Perera, A.; Bartlett, R. J. Reference dependence of the two-determinant coupled-cluster method for triplet and open-shell singlet states of biradical molecules. *The Journal of Chemical Physics* **2018**, *148*, 164102.

[78]Hanauer, M.; Köhn, A. Pilot applications of internally contracted multireference coupled cluster theory, and how to choose the cluster operator properly. *The Journal of Chemical Physics* **2011**, *134*, 204111.

[79]Evangelista, F. A.; Gauss, J. An orbital-invariant internally contracted multireference coupled cluster approach. *The Journal of Chemical Physics* **2011**, *134*, 114102.

[80]Hanauer, M.; Köhn, A. Communication: Restoring full size extensivity in internally contracted multireference coupled cluster theory. *The Journal of Chemical Physics* **2012**, *137*, 131103.

[81]Datta, D.; Kong, L.; Nooijen, M. A state-specific partially internally contracted multireference coupled cluster approach. *The Journal of Chemical Physics* **2011**, *134*, 214116.

[82]Li, S. Block-correlated coupled cluster theory: The general formulation and its application to the antiferromagnetic Heisenberg model. *The Journal of Chemical Physics* **2004**, *120*, 5017–5026.

[83]Evangelista, F. A.; Gauss, J. Insights into the orbital invariance problem in state-specific multireference coupled cluster theory. *The Journal of Chemical Physics* **2010**, *133*, 044101.

[84]Kong, L. Orbital invariance issue in multireference methods. *International Journal of Quantum Chemistry* **2010**, *110*, 2603–2613.

[85]Neuscamman, E.; Yanai, T.; Chan, G. K.-L. Strongly contracted canonical transformation theory. *The Journal of Chemical Physics* **2010**, *132*, 024106.

[86]Neuscamman, E.; Yanai, T.; Chan, G. K.-L. A review of canonical transformation theory. *International Reviews in Physical Chemistry* **2010**, *29*, 231–271.

[87]Oliphant, N.; Adamowicz, L. Multireference coupled-cluster method using a single-reference formalism. *The Journal of Chemical Physics* **1991**, *94*, 1229–1235.

[88]Piecuch, P.; Kucharski, S. A.; Bartlett, R. J. Coupled-cluster methods with internal and semi-internal triply and quadruply excited clusters: CCSD t and CCSD tq approaches. *The Journal of Chemical Physics* **1999**, *110*, 6103–6122.

[89]Shen, J.; Piecuch, P. Combining active-space coupled-cluster methods with moment energy corrections via the CC (P; Q) methodology, with benchmark calculations for biradical transition states. *The Journal of Chemical Physics* **2012**, *136*, 144104.

[90]Bauman, N. P.; Shen, J.; Piecuch, P. Combining active-space coupled-cluster approaches with moment energy corrections via the CC (P; Q) methodology: connected quadruple excitations. *Molecular Physics* **2017**, *115*, 2860–2891.

[91]Piecuch, P.; Oliphant, N.; Adamowicz, L. A state-selective multireference coupled-cluster theory employing the single-reference formalism. *The Journal of Chemical Physics* **1993**, *99*, 1875–1900.

[92]Adamowicz, L.; Malrieu, J.-P.; Ivanov, V. V. New approach to the state-specific multireference coupled-cluster formalism. *The Journal of Chemical Physics* **2000**, *112*, 10075–10084.

[93]Lyakh, D. I.; Ivanov, V. V.; Adamowicz, L. A generalization of the state-specific complete-active-space coupled-cluster method for calculating electronic excited states. *The Journal of Chemical Physics* **2008**, *128*, 074101.

[94]Deustua, J. E.; Shen, J.; Piecuch, P. Converging high-level coupled-cluster energetics by Monte Carlo sampling and moment expansions. *Physical Review Letters* **2017**, *119*, 223003.

[95]Deustua, J. E.; Magoulas, I.; Shen, J.; Piecuch, P. Communication: Approaching exact quantum chemistry by cluster analysis of full configuration interaction quantum Monte Carlo wave functions. *The Journal of Chemical Physics* **2018**, *149*, 151101.

[96]Crawford, T. D.; Schaefer III, H. F. An introduction to coupled cluster theory for computational chemists. *Reviews in Computational Chemistry* **2007**, *14*, 33–136.

[97]Helgaker, T.; Jorgensen, P.; Olsen, J. *Molecular electronic-structure theory*; John Wiley & Sons: New York, 2013.

[98]Martin, R. L. Natural transition orbitals. *The Journal of Chemical Physics* **2003**, *118*, 4775–4777.

[99]Park, Y. C.; Perera, A.; Bartlett, R. J. Low scaling EOM-CCSD and EOM-MBPT (2) method with natural transition orbitals. *The Journal of Chemical Physics* **2018**, *149*, 184103.

[100]Pulay, P. Convergence acceleration of iterative sequences. The case of SCF iteration. *Chemical Physics Letters* **1980**, *73*, 393–398.

[101]Goldstone, J. Derivation of the Brueckner many-body theory. *Proceedings of the Royal Society of London. Series A. Mathematical and Physical Sciences* **1957**, *239*, 267–279.

[102]Bartlett, R. J.; Purvis, G. D. Many-body perturbation theory, coupled-pair many-electron theory, and the importance of quadruple excitations for the correlation problem. *International Journal of Quantum Chemistry* **1978**, *14*, 561–581.

[103]Piecuch, P.; Włoch, M.; Gour, J. R.; Kinal, A. Single-reference, size-extensive, non-iterative coupled-cluster approaches to bond breaking and biradicals. *Chemical Physics Letters* **2006**, *418*, 467–474.

[104]Piecuch, P.; Włoch, M. Renormalized coupled-cluster methods exploiting left eigenstates of the similarity-transformed Hamiltonian. *The Journal of Chemical Physics* **2005**, *123*, 224105.

[105]Piecuch, P.; Hansen, J. A.; Ajala, A. O. Benchmarking the completely renormalised equation-of-motion coupled-cluster approaches for vertical excitation energies. *Molecular Physics* **2015**, *113*, 3085–3127.

[106]Piecuch, P.; Kucharski, S. A.; Kowalski, K.; Musiał, M. Efficient computer implementation of the renormalized coupled-cluster methods: the r-ccsd [t], r-ccsd (t), cr-ccsd [t], and cr-ccsd (t) approaches. *Computer Physics Communications* **2002**, *149*, 71–96.

[107]Kowalski, K.; Piecuch, P. New coupled-cluster methods with singles, doubles, and noniterative triples for high accuracy calculations of excited electronic states. *The Journal of Chemical Physics* **2004**, *120*, 1715–1738.

[108]Piecuch, P.; Gour, J. R.; Włoch, M. Left-eigenstate completely renormalized equation-of-motion coupled-cluster methods: Review of key concepts, extension to excited states of open-shell systems, and comparison with electron-attached and ionized approaches. *International Journal of Quantum Chemistry* **2009**, *109*, 3268–3304.

[109]Fradelos, G.; Lutz, J. J.; Wesołowski, T. A.; Piecuch, P.; Włoch, M. Embedding vs supermolecular strategies in evaluating the hydrogen-bonding-induced shifts of excitation energies. *Journal of Chemical Theory and Computation* **2011**, *7*, 1647–1666.

[110]Schmidt, M. W.; Baldridge, K. K.; Boatz, J. A.; Elbert, S. T.; Gordon, M. S.; Jensen, J. H.; Koseki, S.; Matsunaga, N.; Nguyen, K. A.; Su, S.; Windus, T. L.; Dupuis, M.; Montgomery Jr, J. A. General atomic and molecular electronic structure system. *Journal of Computational Chemistry* **1993**, *14*, 1347–1363.

[111]Barca, G. M. et al. Recent developments in the general atomic and molecular electronic structure system. *The Journal of Chemical Physics* **2020**, *152*, 154102.

[112]Sun, Q. Libcint: An efficient general integral library for gaussian basis functions. *Journal of Computational Chemistry* **2015**, *36*, 1664–1671.

[113]Sun, Q.; Berkelbach, T. C.; Blunt, N. S.; Booth, G. H.; Guo, S.; Li, Z.; Liu, J.; McClain, J. D.; Sayfutyarova, E. R.; Sharma, S.; Wouters, S.; Chan, G. K.-L. PySCF: the Python-based simulations of chemistry framework. *Wiley Interdisciplinary Reviews: Computational Molecular Science* **2018**, *8*, e1340.

[114]Sun, Q. et al. Recent developments in the PySCF program package. *The Journal of Chemical Physics* **2020**, *153*, 024109.

VII. SUPPORTING INFORMATION

S1. RELEVANT PROOFS

A. Intermediate Normalization

$$\langle\psi_0|\Psi\rangle = \frac{1}{\sqrt{2}}\left(\langle\phi^{*p}_h|\,\hat{P}e^{\hat{T}}\,|\phi^*_0\rangle + \langle\phi^{*\bar{p}}_{\bar{h}}|\,\hat{P}e^{\hat{T}}\,|\phi^*_0\rangle\right) \tag{S1}$$

$$= \frac{1}{\sqrt{2}}\left(\langle\phi^{*p}_h|\,\hat{P}(1+\hat{T}+\dots)\,|\phi^*_0\rangle + \langle\phi^{*\bar{p}}_{\bar{h}}|\,\hat{P}(1+\hat{T}+\dots)\,|\phi^*_0\rangle\right) \tag{S2}$$

$$= \frac{1}{\sqrt{2}}\left(t^p_h + t^{\bar{p}}_{\bar{h}}\right) = 1 \tag{S3}$$

$$\langle\psi_0|\,e^{-\hat{T}}\,|\Psi\rangle = \frac{1}{\sqrt{2}}\left(\langle\phi^{*p}_h|\,e^{-\hat{T}}\hat{P}e^{\hat{T}}\,|\phi^*_0\rangle + \langle\phi^{*\bar{p}}_{\bar{h}}|\,e^{-\hat{T}}\hat{P}e^{\hat{T}}\,|\phi^*_0\rangle\right) \tag{S4}$$

$$= \frac{1}{\sqrt{2}}\Big(\langle\phi^{*p}_h|\,(1-\hat{T}+\dots)\hat{P}(1+\hat{T}+\dots)\,|\phi^*_0\rangle \tag{S5}$$

$$+ \langle\phi^{*\bar{p}}_{\bar{h}}|\,(1-\hat{T}+\dots)\hat{P}(1+\hat{T}+\dots)\,|\phi^*_0\rangle\Big)$$

$$= \frac{1}{\sqrt{2}}\Big(\langle\phi^{*p}_h|\,\hat{P}(1+\hat{T}+\dots)\,|\phi^*_0\rangle + \langle\phi^{*\bar{p}}_{\bar{h}}|\,\hat{P}(1+\hat{T}+\dots)\,|\phi^*_0\rangle \tag{S6}$$

$$-t^p_h\,\langle\phi^*{}_0|\,\hat{P}(1+\hat{T}+\dots)\,|\phi^*_0\rangle - t^{\bar{p}}_{\bar{h}}\,\langle\phi^*{}_0|\,\hat{P}(1+\hat{T}+\dots)\,|\phi^*_0\rangle\Big)$$

$$= \frac{1}{\sqrt{2}}\left(t^p_h + t^{\bar{p}}_{\bar{h}}\right) = 1 \tag{S7}$$

B. Size Intensivity of Energy

$$\frac{\langle\psi_0|\,e^{-\hat{T}}\hat{H}\hat{P}e^{\hat{T}}\,|\phi^*_0\rangle}{\langle\psi_0|\,e^{-\hat{T}}\hat{P}e^{\hat{T}}\,|\phi^*_0\rangle} = \frac{1}{\sqrt{2}}\left(\langle\phi^{*p}_h|\,e^{-\hat{T}}\hat{H}\hat{P}e^{\hat{T}}\,|\phi^*_0\rangle + \langle\phi^{*\bar{p}}_{\bar{h}}|\,e^{-\hat{T}}\hat{H}\hat{P}e^{\hat{T}}\,|\phi^*_0\rangle\right) \tag{S8}$$

$$= \frac{1}{\sqrt{2}}\Big[(\langle\phi^{*\,p}_{Ah}|\otimes\langle\phi^*_B|)\left(e^{-\hat{T}_A}\otimes e^{-\hat{T}_B}\right)\left(\hat{H}_A+\hat{H}_B\right)\hat{P}_A\left(e^{\hat{T}_A}\otimes e^{\hat{T}_B}\right)(|\phi^*_A\rangle\otimes|\phi^*_B\rangle) \tag{S9}$$

$$+ \left(\langle\phi^{*\,\bar{p}}_{A\bar{h}}|\otimes\langle\phi^*_B|\right)\left(e^{-\hat{T}_A}\otimes e^{-\hat{T}_B}\right)\left(\hat{H}_A+\hat{H}_B\right)\hat{P}_A\left(e^{\hat{T}_A}\otimes e^{\hat{T}_B}\right)(|\phi^*_A\rangle\otimes|\phi^*_B\rangle)\Big]$$

$$= \frac{1}{\sqrt{2}}\Big[\langle\phi^{*\,p}_{Ah}|\,e^{-\hat{T}_A}\hat{H}_A\hat{P}_Ae^{\hat{T}_A}\,|\phi^*_A\rangle\otimes\langle\phi^*_B|\,e^{-\hat{T}_B}e^{\hat{T}_B}\,|\phi^*_B\rangle \tag{S10}$$

$$+ \langle\phi^{*\,p}_{Ah}|\,e^{-\hat{T}_A}\hat{P}_Ae^{\hat{T}_A}\,|\phi^*_A\rangle\otimes\langle\phi^*_B|\,e^{-\hat{T}_B}\hat{H}_Be^{\hat{T}_B}\,|\phi^*_B\rangle$$

$$+ \langle\phi^{*\,\bar{p}}_{A\bar{h}}|\,e^{-\hat{T}_A}\hat{H}_A\hat{P}_Ae^{\hat{T}_A}\,|\phi^*_A\rangle\otimes\langle\phi^*_B|\,e^{-\hat{T}_B}e^{\hat{T}_B}\,|\phi^*_B\rangle$$

$$+ \langle\phi^{*\,\bar{p}}_{A\bar{h}}|\,e^{-\hat{T}_A}\hat{P}_Ae^{\hat{T}_A}\,|\phi^*_A\rangle\otimes\langle\phi^*_B|\,e^{-\hat{T}_B}\hat{H}_Be^{\hat{T}_B}\,|\phi^*_B\rangle\Big]$$

$$= \frac{1}{\sqrt{2}}\Big[\langle\phi^{*\,p}_{Ah}|\,e^{-\hat{T}_A}\hat{H}_A\hat{P}_Ae^{\hat{T}_A}\,|\phi^*_A\rangle + \langle\phi^{*\,p}_{Ah}|\,e^{-\hat{T}_A}\hat{P}_Ae^{\hat{T}_A}\,|\phi^*_A\rangle\otimes\langle\phi^*_B|\,e^{-\hat{T}_B}\hat{H}_Be^{\hat{T}_B}\,|\phi^*_B\rangle \tag{S11}$$

$$+ \langle\phi^{*\,\bar{p}}_{A\bar{h}}|\,e^{-\hat{T}_A}\hat{H}_A\hat{P}_Ae^{\hat{T}_A}\,|\phi^*_A\rangle + \langle\phi^{*\,\bar{p}}_{A\bar{h}}|\,e^{-\hat{T}_A}\hat{P}_Ae^{\hat{T}_A}\,|\phi^*_A\rangle\otimes\langle\phi^*_B|\,e^{-\hat{T}_B}\hat{H}_Be^{\hat{T}_B}\,|\phi^*_B\rangle\Big]$$

$$= \frac{1}{\sqrt{2}}\Big[\langle\phi^{*\,p}_{Ah}|\,e^{-\hat{T}_A}\hat{H}_A\hat{P}_Ae^{\hat{T}_A}\,|\phi^*_A\rangle + \langle\phi^{*\,\bar{p}}_{A\bar{h}}|\,e^{-\hat{T}_A}\hat{H}_A\hat{P}_Ae^{\hat{T}_A}\,|\phi^*_A\rangle\Big] \tag{S12}$$

$$+ \langle\phi^*_B|\,e^{-\hat{T}_B}\hat{H}_Be^{\hat{T}_B}\,|\phi^*_B\rangle$$

$$= \langle\psi_{0\,A}|\,e^{-\hat{T}_A}\hat{H}_A\hat{P}_Ae^{\hat{T}_A}\,|\phi^*_A\rangle + \langle\phi^*_B|\,e^{-\hat{T}_B}\hat{H}_Be^{\hat{T}_B}\,|\phi^*_B\rangle = E_A + E_B = E \tag{S13}$$

C. Factorizability of Amplitude Equations

$$\langle \phi^{*\,pb}_{\;hj}| \, e^{-\hat{T}} \left(\hat{H} - E\right) \hat{P} e^{\hat{T}} \, |\phi^*_0\rangle \tag{S14}$$

$$= \left(\langle \phi^{*\,p}_{Ah}| \otimes \langle \phi^{*\,b}_{Bj}|\right) \left(e^{-\hat{T}_A} \otimes e^{-\hat{T}_B}\right) \left(\hat{H}_A + \hat{H}_B - E\right) \hat{P}_A \left(e^{\hat{T}_A} \otimes e^{\hat{T}_B}\right) (|\phi^*_A\rangle \otimes |\phi^*_B\rangle) \tag{S15}$$

$$= \langle \phi^{*\,p}_{Ah}| \, e^{-\hat{T}_A} \left(\hat{H}_A - E\right) \hat{P}_A e^{\hat{T}_A} \, |\phi^*_A\rangle \otimes \langle \phi^{*\,b}_{Bj}| \, e^{-\hat{T}_B} e^{\hat{T}_B} \, |\phi^*_B\rangle \tag{S16}$$

$$+ \langle \phi^{*\,p}_{Ah}| \, e^{-\hat{T}_A} \hat{P}_A e^{\hat{T}_A} \, |\phi^*_A\rangle \otimes \langle \phi^{*\,b}_{Bj}| \, e^{-\hat{T}_B} \hat{H}_B e^{\hat{T}_B} \, |\phi^*_B\rangle$$

$$= \langle \phi^{*\,p}_{Ah}| \, e^{-\hat{T}_A} \hat{P}_A e^{\hat{T}_A} \, |\phi^*_A\rangle \otimes \langle \phi^{*\,b}_{Bj}| \, e^{-\hat{T}_B} \hat{H}_B e^{\hat{T}_B} \, |\phi^*_B\rangle \tag{S17}$$

$$= \langle \phi^{*\,p}_{Ah}| \left(1 - \hat{T}_A + \dots\right) \hat{P}_A \left(1 + \hat{T}_A + \dots\right) |\phi^*_A\rangle \otimes \langle \phi^{*\,b}_{Bj}| \, e^{-\hat{T}_B} \hat{H}_B e^{\hat{T}_B} \, |\phi^*_B\rangle \tag{S18}$$

$$= \left[\langle \phi^{*\,p}_{Ah}| \, \hat{P}_A \left(1 + \hat{T}_A\right) |\phi^*_A\rangle - t^p_h \, \langle \phi^*_A| \, \hat{P}_A \left(1 + \hat{T}_A\right) |\phi^*_A\rangle\right] \otimes \langle \phi^{*\,b}_{Bj}| \, e^{-\hat{T}_B} \hat{H}_B e^{\hat{T}_B} \, |\phi^*_B\rangle \tag{S19}$$

$$= \left[t^p_h \langle \phi^{*\,p}_{Ah}| \, \hat{P}_A \, |\phi^{*\,a}_{Ai}\rangle - t^p_h \langle \phi^*_A| \, \hat{P}_A \, |\phi^*_A\rangle\right] \otimes \langle \phi^{*\,b}_{Bj}| \, e^{-\hat{T}_B} \hat{H}_B e^{\hat{T}_B} \, |\phi^*_B\rangle \tag{S20}$$

$$= t^p_h \, \langle \phi^{*\,b}_{Bj}| \, e^{-\hat{T}_B} \hat{H}_B e^{\hat{T}_B} \, |\phi^*_B\rangle \tag{S21}$$

$$\langle \phi^{*\,pbc}_{\;hjk}| \, e^{-\hat{T}} \left(\hat{H} - E\right) \hat{P} e^{\hat{T}} \, |\phi^*_0\rangle \tag{S22}$$

$$= \left(\langle \phi^{*\,p}_{Ah}| \otimes \langle \phi^{*\,bc}_{Bjk}|\right) \left(e^{-\hat{T}_A} \otimes e^{-\hat{T}_B}\right) \left(\hat{H}_A + \hat{H}_B - E\right) \hat{P}_A \left(e^{\hat{T}_A} \otimes e^{\hat{T}_B}\right) (|\phi^*_A\rangle \otimes |\phi^*_B\rangle) \tag{S23}$$

$$= \langle \phi^{*\,p}_{Ah}| \, e^{-\hat{T}_A} \left(\hat{H}_A - E\right) \hat{P}_A e^{\hat{T}_A} \, |\phi^*_A\rangle \otimes \langle \phi^{*\,bc}_{Bjk}| \, e^{-\hat{T}_B} e^{\hat{T}_B} \, |\phi^*_B\rangle \tag{S24}$$

$$+ \langle \phi^{*\,p}_{Ah}| \, e^{-\hat{T}_A} \hat{P}_A e^{\hat{T}_A} \, |\phi^*_A\rangle \otimes \langle \phi^{*\,bc}_{Bjk}| \, e^{-\hat{T}_B} \hat{H}_B e^{\hat{T}_B} \, |\phi^*_B\rangle$$

$$= \langle \phi^{*\,p}_{Ah}| \, e^{-\hat{T}_A} \hat{P}_A e^{\hat{T}_A} \, |\phi^*_A\rangle \otimes \langle \phi^{*\,bc}_{Bjk}| \, e^{-\hat{T}_B} \hat{H}_B e^{\hat{T}_B} \, |\phi^*_B\rangle \tag{S25}$$

$$= \langle \phi^{*\,p}_{Ah}| \left(1 - \hat{T}_A + \dots\right) \hat{P}_A \left(1 + \hat{T}_A + \dots\right) |\phi^*_A\rangle \otimes \langle \phi^{*\,bc}_{Bjk}| \, e^{-\hat{T}_B} \hat{H}_B e^{\hat{T}_B} \, |\phi^*_B\rangle \tag{S26}$$

$$= \left[\langle \phi^{*\,p}_{Ah}| \, \hat{P}_A \left(1 + \hat{T}_A\right) |\phi^*_A\rangle - t^p_h \, \langle \phi^*_A| \, \hat{P}_A \left(1 + \hat{T}_A\right) |\phi^*_A\rangle\right] \otimes \langle \phi^{*\,bc}_{Bjk}| \, e^{-\hat{T}_B} \hat{H}_B e^{\hat{T}_B} \, |\phi^*_B\rangle \tag{S27}$$

$$= \left[t^p_h \langle \phi^{*\,p}_{Ah}| \, \hat{P}_A \, |\phi^{*\,p}_{Ah}\rangle - t^p_h \langle \phi^*_A| \, \hat{P}_A \, |\phi^*_A\rangle\right] \otimes \langle \phi^{*\,bc}_{Bjk}| \, e^{-\hat{T}_B} \hat{H}_B e^{\hat{T}_B} \, |\phi^*_B\rangle \tag{S28}$$

$$= t^p_h \, \langle \phi^{*\,bc}_{Bjk}| \, e^{-\hat{T}_B} \hat{H}_B e^{\hat{T}_B} \, |\phi^*_B\rangle \tag{S29}$$

S2. MOLECULAR GEOMETRIES

All geometries are reported in Bohr.

H_6

```
H  0.000000000 -0.900000000  0.000000000
H  0.000000000  0.900000000  0.000000000
H  7.000000000  0.200000000  0.000000000
H  8.400000000  0.200000000  0.050000000
H -7.000000000 -0.200000000  0.050000000
H -8.400000000 -0.200000000  0.000000000
```

Water

```
O  0.000000000  0.000000000 -0.112851412
H  0.000000000  1.425999575  0.970077421
H  0.000000000 -1.425999575  0.970077421
```

Formaldehyde

```
C  0.000000000  0.000000000 -1.126692899
O  0.000000000  0.000000000  1.111413933
H  0.000000000  1.746571764 -2.224070962
H  0.000000000 -1.746571764 -2.224070962
```

Ketene

```
C  0.000000000  0.000000000 -2.433659698
C  0.000000000  0.000000000  0.034004982
O  0.000000000  0.000000000  2.198008243
H  0.000000000  1.764688153 -3.424475103
H  0.000000000 -1.764688153 -3.424475103
```

Ammonia → Difluorine

```
N  0.000000000 -0.443921233 -6.652831844
H  0.000000000  1.331763699 -7.379272802
H  1.537789200 -1.331763699 -7.379272802
H -1.537789200 -1.331763699 -7.379272802
F  0.000000000 -0.443921233  4.685524903
F  0.000000000 -0.443921233  7.379272802
```

Neon

```
Ne  0.000000000  0.000000000  0.000000000
```